IIETA International Information and Engineering Technology Association
Advancing the World of Information and Engineering

Journal Européen des Systèmes Automatisés
Vol. 58, No. 10, October, 2025, pp. 2143-2152
Journal homepage: http://iieta.org/journals/jesa

Full-State Feedback H-Infinity Controller Design for Nonlinear Systems with Uncertainties Using PSO

Ahmed L. Jassim[1*], Hazem I. Ali[2], Omar F. Lutfy[1]

[1] Control and System Engineering Department, University of Technology, Baghdad 10011, Iraq
[2] Electrical Engineering Department, University of Technology, Baghdad 10011, Iraq

Corresponding Author Email: cse.22.01@grad.uotechnology.edu.iq

https://doi.org/10.18280/jesa.581014

Received: 22 June 2025
Revised: 8 August 2025
Accepted: 10 September 2025
Available online: 31 October 2025

Keywords:
robust controller, state feedback, H-infinity controller, particle swarm algorithm

ABSTRACT

This study develops a robust control approach employing full-state feedback within the H-infinity framework to manage nonlinear dynamic systems influenced by parameter variations and external perturbations The control design involves formulating the H-infinity optimization challenge and resolving the corresponding algebraic Riccati equation to derive the optimal gain matrix. To improve the controller's effectiveness and facilitate automatic tuning, the Particle Swarm Optimization (PSO) algorithm is utilized as a powerful metaheuristic optimizer for selecting the best H-infinity design parameters. The controller's implementation and performance validation are conducted through MATLAB simulations. Two distinct categories of nonlinear systems serve as benchmarks to assess the proposed method. The simulation outcomes confirm that the PSO-optimized H-infinity controller significantly enhances system stability and tracking robustness, maintaining reliable performance despite uncertainties in the model.

1. INTRODUCTION

Nonlinear dynamical systems are widely encountered across diverse engineering fields, such as robotics, aerospace, and electrical power networks. Their inherent characteristics including multiple equilibrium points, the potential for limit cycle behavior, and heightened sensitivity to parameter changes and external perturbations-pose significant challenges to the design of effective control strategies.

Robust control theory provides a framework to design controllers that maintain desired performance levels despite uncertainties and disturbances. Among robust control techniques, the H-infinity control method has gained prominence for its ability to minimize the maximum gain under worst-case disturbance conditions to system outputs, ensuring robustness against uncertainties in the system model and disturbances originating from external sources [1, 2].

In the context of state feedback H-infinity control, the controller utilizes full access to the system's dynamic states as the basis for determining the appropriate control signal. This approach involves solving an algebraic Riccati equation (ARE) derived from the system's dynamics to obtain the optimal gain matrix. However, determining appropriate weighting parameters and solving the ARE can be computationally intensive, especially for nonlinear systems [3].

To address these challenges, metaheuristic optimization techniques such as Particle Swarm Optimization (PSO) have been employed. PSO operates as an optimization technique that relies on a population of candidate solutions inspired by the social behavior of birds and fish, known for its simplicity, fast convergence, and global search capability. Recent studies have demonstrated the effectiveness of PSO in tuning H-infinity controller parameters, leading to improved performance and robustness in nonlinear systems [4, 5].

This investigation employs a Particle Swarm Optimization (PSO) algorithm to optimize the gain matrix of an H-infinity full-state feedback controller. This methodology synergistically combines the inherent robustness characteristics of H-infinity control with the adaptive optimization capabilities of PSO. The primary objective is to enhance overall system performance, specifically in terms of improved reference tracking accuracy and superior disturbance attenuation capabilities. The controller design is carried out using MATLAB, and its performance is verified through simulation tests on two different nonlinear dynamic models.

The structure of the paper is outlined as follows: initially, the Particle Swarm Optimization (PSO) algorithm is presented, emphasizing its integration into the controller development process. Subsequently, the fundamentals of H-infinity control using full-state feedback are discussed, including the formulation of the Riccati-based control law.

The structure of the proposed optimization-based controller is then outlined, including the selection and tuning of design parameters within the PSO algorithm. The subsequent section presents simulation outcomes for two representative nonlinear system models, employed as case studies to evaluate the proposed controller's performance and robustness in the presence of uncertainties. The paper concludes with a synthesis of the key results and recommendations for potential avenues of future investigation.

2. PARTICLE SWARM OPTIMIZATION (PSO)

The Particle Swarm Optimization (PSO) algorithm employs particles as representations of individual solutions within a population. Each particle navigates within a multi-dimensional search space, with its velocity continuously updated. This update mechanism relies on the particle's own historical experience, as well as the collective experience gained from neighboring particles, or, in some instances, the entire swarm. This approach has demonstrated successful efficacy across various application domains [6].

Specifically, the implementation of the PSO algorithm proceeds as follows:

1. Initialization of Particles: The individual solutions are considered as particles, forming a population of size n.
2. Stochastic Initialization and Exploration: The particles are initially assigned random positions within the search space and then proceed to explore the space in order to minimize a given objective function.
3. Minimization of the Objective Function: The algorithm systematically minimizes the objective function to optimize the problem parameters.
4. Fitness Evaluation: Each particle's fitness is assessed using the defined objective function, allowing the identification of both the particle's own best-known position ($X_p best$) and the overall best position found by the entire swarm ($X_g best$).
5. Attraction Toward Optimal Solutions: Each particle's movement is guided by a combination of its personal best location attained so far and the globally optimal location discovered by the swarm. This dual influence guides the swarm toward more favorable areas within the search domain, thereby enhancing convergence toward optimal or near-optimal solutions [7].

The update rule for Velocity corresponding to the i^{th} particle, denoted by v_i, is given by the Eq. (1) below, which incorporates both cognitive and social components of the PSO algorithm.

$$v_i(k+1) = \mathrm{X}(v_i(k) + c_{m1} r_{m1}\Big(\big(pbest_i(k) - x_i(k)\big) + c_{m2} r_{m2}\big(gbest - x_i(k)\big)\Big) \quad (1)$$

At the k^{th} iteration, the position of the i^{th} particle is denoted by x_i, while $(pbest_i)$ represents its personal best position achieved thus far, and $(gbest)$ corresponds to the best position identified across the entire swarm. The acceleration coefficients (c_{m1}) and (c_{m2}) reflect the cognitive and social influences, respectively, guiding the particle's trajectory based on both individual performance and collective knowledge.

In addition, (r_{m1}) and (r_{m2}) are two arbitrary integers between 0 and 1, and the constriction coefficient (X) is defined as follows [8]:

$$\chi = \frac{2}{\left|4-\phi-\sqrt{\phi^2-4\phi}\right|} \quad (2)$$

where, ($\phi = c_{m1} + c_{m2}$ with the condition $\phi > 4$). Which is imposed to prevent divergence and ensure convergence of the algorithm. Based on this condition, the new position of the i^{th} particle's is updated according to the following Eq. (3) [9]:

$$x_i(k+1) = x_i(k) + v_i(k+1) \quad (3)$$

Particle velocity as defined in the standard Particle Swarm Optimization framework is computed using the following Eq. (4): [6]

$$v_i(k+1) = v_i(k) + c_{m1} r_{m1}\big(\big(pbest_i(k) - x_i(k)\big) + c_{m2} r_{m2}\big(gbest - x_i(k)\big) \quad (4)$$

By incorporating the inertia weight factor ($w \geq 0$), which modulates the influence of previous velocities, Eq. (1) is scaled accordingly, thereby resulting in an adjusted equation for computing the velocity:

$$v_i(k+1) = w\, v_i(k) + c_{m1} r_{m1}\big(\big(pbest_i(k) - x_i(k)\big) + c_{m2} r_{m2}\big(gbest - x_i(k)\big) \quad (5)$$

Prior studies involving PSO algorithms with an inertia weight component have shown that assigning a higher value to the inertia factor (w) promotes broader exploration of the search space, while a lower (w) typically facilitates faster convergence rates [6].

The PSO process terminates once it either fulfills the set limit on iteration count or achieves an acceptable objective function value. If the best cost remains unchanged over successive iterations, this stagnation typically suggests convergence to a global or near-global optimum [10, 11]. One of the key advantages of the PSO methodology lies in its simple and intuitive structure, which makes it easy to implement.

3. DESIGN OF THE CONTROLLER

The proposed control methodology is introduced in this section, targeting dynamical systems described by the general structure shown below. The design is constructed in accordance with the model formulation outlined in the studies [12, 13].

$$\begin{aligned} \dot{x} &= Ax + B_1 d(t) + B_2 u(t) \\ e(t) &= C_1 x + D_{12} u(t) \\ y &= C_2 x \end{aligned} \quad (6)$$

where, $x \in R^n$ represents the system state vector, $d(t) \in R^m$ denotes the external disturbance, $u(t) \in R^l$ is the control input. The variable $e(t) \in R^q$ indicates the controlled output, while $y \in R^p$ corresponds to the measured output, which is assumed to be fully available for feedback. The system matrices are defined as follows: A, B_1 and B_2 have dimensions $n \times n, n \times m,$ and $n \times l$ respectively, and are elements of the real number space. Moreover $C_1 \in R^{q \times n}, D_{12} \in R^{q \times l}$ are weighting matrices associated with the state and control input penalties, respectively, while $C_2 \in R^{p \times n}$ defines the matrix weighting the system output.

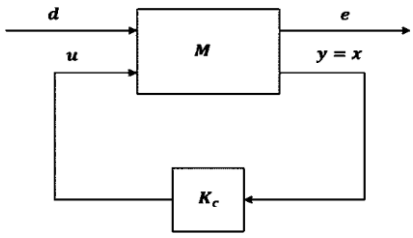

Figure 1. Block diagram of the full-state feedback H-infinity control system

Figure 1 illustrates the conventional setup of the full-state feedback H-infinity control framework. In this diagram, the symbol *M* represents the augmented plant, which incorporates both the core system dynamics and the associated performance and disturbance pathways [13].

$$M = \begin{bmatrix} A & B_1 & B_2 \\ C_1 & D_{11} & D_{12} \\ C_2 & D_{21} & D_{22} \end{bmatrix} \tag{7}$$

For the successful deployment of a full-state feedback H-infinity control strategy, it is imperative that the entire state vector of the system is observable and accessible for feedback control. This requirement leads to the following assumptions: $C_2 = I. D_{11}, D_{21}\ and\ D_{22} = 0$. Under these conditions, the structure of the augmented plant matrix M is simplified accordingly, resulting in the following representation:

$$M = \begin{bmatrix} A & B_1 & B_2 \\ C_1 & 0 & D_{12} \\ I & 0 & 0 \end{bmatrix} \tag{8}$$

The construction of the H-infinity state feedback controller presupposes several fundamental assumptions, specifically:
(1) The system pair $(A, B_1) and\ (A, B_2)$ exhibit stabilizability.
(2) The detectability condition is satisfied by the pair (C_1, A)
(3) Additionally, the matrix conditions $C_1^T D_{12}$ equals zero and $D_{12}^T D_{12}^T$ equals the identity matrix are assumed to hold.

It should be emphasized that the application of this control technique to a nonlinear system requires reformulating the system into a structure that aligns with the form defined in Eq. (6). A transformation of the state variables is employed to ensure that nonlinearities and uncertainties, often regarded as problematic terms, are mapped onto the same pathway influenced by the control input *u*. This alignment satisfies the matching condition, thereby allowing the controller to neutralize their effect more effectively. A diffeomorphic mapping $T: D \rightarrow R^n$, is utilized to convert the system from its native coordinate system in $(x - space)$ into a reformulated domain referred to as $(z - space)$, facilitating the analysis and controller design [14].

$$z = T(x) \tag{9}$$

To guarantee the unique reconstruction of the original system states, the transformation T is required to be invertible and differentiable, ensuring the existence of a well-defined inverse, that is:

$$x = T^{-1}(z) \tag{10}$$

The origin of the transformed system in the z-space remains identical to that of the original system, ensuring consistency under the state transformation [14].

$$T(0) = 0 \tag{11}$$

Through this transformation, the original nonlinear system is reformulated into the following canonical structure [15]:

$$\dot{z} = Az + B_1 d(t) + B_2 u(t) \tag{12}$$

The central objective of the control design is to derive an optimal control input u^*, which depends on the system states and guarantees the internal stability of the closed-loop system. This is accomplished by constraining the H-infinity measure associated with transfer function T_{ed} under the closed-loop to remain below a specified performance threshold γ, as detailed in the subsequent formulation [12]:

$$\|T_{ed}(s)\|_\infty < \gamma \tag{13}$$

in this context, γ represents the maximum allowable level of disturbances and uncertainties that the control input can effectively attenuate. The criterion outlined in Eq.(13) consequently, leads to the following condition [13]:

$$\underset{u}{inf}\ \underset{d}{sup}\ J(u, d) < \infty \tag{14}$$

$$J(u, d) = \int_0^\infty (e^T e - \gamma^2 d^T d)\, dt \tag{15}$$

Within the H-infinity control paradigm, an inherent adversarial relationship exists where the disturbance input, denoted as $d(t)$, endeavors to amplify the performance index $J(t)$, while the applied control input $u(t)$, simultaneously strives to reduce it. This fundamental antagonistic interplay is formally conceptualized as a minimax optimization problem, wherein both inputs operate under diametrically opposed objectives. Mathematically, this competitive dynamic is precisely characterized by the application of the The operators representing the greatest lower bound (infimum) and the least upper bound (supremum), denoted as *inf* and *sup*, respectively. Consequently, the corresponding expressions defining the optimal control action and the worst-case disturbance are rigorously established as follows [16]:

$$d(t) = k_d x(t) \tag{16}$$

and

$$u(t) = k_c x(t) \tag{17}$$

by substituting Eq. (17) into Eq. (6), the dynamics of system are reformulated as follows:

$$e(t) = (C_1 + D_{12} k_c) x(t) \tag{18}$$

utilizing Assumption 3, This expression may be reduced to the form shown below:

$$e^T e = x^T (C_1^T C_1 + k_c^T k_c) x \tag{19}$$

Therefore,

$$J = \int_0^\infty x^T (C_1^T C_1 + k_c^T k_c - \gamma^2 k_d^T k_d) x\, dt \tag{20}$$

by incorporating Eqs. (18) and (19) into the structure defined by Eq. (6), the resulting expression becomes:

$$\dot{x} = (A + B_1 k_d + B_2 k_c) x \tag{21}$$

considering the performance metric defined in Eq. (15), define:

$$Q = C_1^T C_1 + k_c^T k_c - \gamma^2 k_d^T k_d \tag{22}$$

where, Q is required to be a positive definite matrix. It is

assumed that the system represented by Eq. (21) remains stable under the optimal control law derived in Eq. (17). Under this assumption, we proceed to define:

$$V(x) = x^T P x \tag{23}$$

and

$$\dot{V}(x) = -x^T Q x \tag{24}$$

In this context, $V(x)$ denotes a quadratic Lyapunov function that is positive definite. To derive the optimal cost expression, Eq. (22) is substituted into Eq. (24), yielding:

$$\dot{V}(x) = -x^T (C_1^T C_1 + k_c^T k_c - \gamma^2 k_d^T k_d) x \tag{25}$$

$$x^T (C_1^T C_1 + k_c^T k_c - \gamma^2 k_d^T k_d) x = -\frac{d}{dt} x^T P x \tag{26}$$

Integrating Eq. (26) over the time interval 0 to ∞, yields the following result:

$$\int_0^\infty x^T (C_1^T C_1 + k_c^T k_c - \gamma^2 k_d^T k_d) x = \int_0^\infty -\frac{d}{dt} x^T P x \tag{27}$$

$$J = -x(\infty)^T P x(\infty) - (x(0)^T P x(0)) \tag{28}$$

Given that the system described by Eq. (21) is stabilized by applying the control law, the system state converges to zero as time approaches infinity, $x(\infty) = 0$. Therefore, the formulation of the optimal cost function is as follows:

$$J^* = -x(0)^T P x(0) \tag{29}$$

The matrix P which is positive definite, serves as the solution obtained from the Lyapunov equation below:

$$(A + B_1 k_d + B_2 k_c)^T P + P(A + B_1 k_d + B_2 k_c) = -Q \tag{30}$$

$$(A + B_1 k_d + B_2 k_c)^T P + P(A + B_1 k_d + B_2 k_c) = -(C_1^T C_1 + k_c^T k_c - \gamma^2 k_d^T k_d) \tag{31}$$

$$(A + B_1 k_d + B_2 k_c)^T P + P(A + B_1 k_d + B_2 k_c) - (C_1^T C_1 + k_c^T k_c - \gamma^2 k_d^T k_d) = 0 \tag{32}$$

To determine the optimal control gain, Eq. (32) is differentiated with respect to k_c and by imposing the condition $\frac{\partial P}{\partial k_{c_{ij}}} = 0$, the following expression is obtained:

$$k_c = -{B_2}^T P \tag{33}$$

As a result,

$$u^* = k_c x \xrightarrow{yields} u = -{B_2}^T P x \tag{34}$$

Following the same approach, the worst-case disturbance input is derived by taking the derivative of the Lyapunov equation with respect to k_d, and applying the condition $\frac{\partial P}{\partial k_{d_{ij}}} = 0$, resulting in:

$$k_d = \frac{1}{\gamma^2} {B_1}^T P \tag{35}$$

and

$$d^* = k_d x \xrightarrow{yields} d = \frac{1}{\gamma^2} {B_1}^T P x \tag{36}$$

The Lyapunov equation corresponding to the optimal control configuration and the worst-case disturbance scenario is formulated as:

$$PA + A^T P + C_1^T C_1 - P\left(B_2 {B_2}^T - \frac{1}{\gamma^2} B_1 {B_1}^T\right) P = 0 \tag{37}$$

This expression is referred to as the H-infinity Algebraic Riccati Equation (ARE). The performance requirement $\|T_{ed}(s)\|_\infty < \gamma$ is fulfilled if the following condition holds:

1- The optimal control input $u^* = k_c x = -{B_2}^T P x$.
2- Symmetric positive definite matrix $P > 0$.

Stability of the matrix $A + B_1 k_d + B_2 k_c$ ensures that the matrix $A + B_2 k_c$ is also asymptotically stable.

4. PARAMETER ADJUSTMENT FOR H-INFINITY CONTROLLER

procedure is executed in an offline setup, where complete problem information is provided in advance, allowing the algorithm to search for an optimal solution that addresses the controller design requirements. The Particle Swarm Optimization technique is well-suited for this purpose due to its simplicity and proven effectiveness in high-dimensional optimization problems. In the proposed method, PSO algorithm is applied to determine the best values for both the elements of the matrix C_1 (as given in Eq. (6)) and the performance bound of γ (from Eq. (37)). This optimization process is designed to achieve robust system stability while meeting the desired performance criteria. To measure and improve the system's time-domain response, the performance criterion is based on the Integral of the Squared Error (ISE).

Figure 2 illustrates the block diagram of the control framework enhanced with a PSO-driven optimization mechanism. Within this structure, the PSO algorithm explores the predefined search space to identify the controller parameters that minimize the ISE while ensuring compliance with the H-infinity performance requirement specified in Eq. (37). To facilitate the robust synthesis of the controller via PSO, the following configuration parameters were employed:

1. The optimization process focuses on identifying the optimal values for the decision variables, which include the elements $c_{11}, c_{12}, \dots, c_{nn}$ of the matrix C_1 in addition to the performance bound γ.
2. The PSO algorithm is configured with a swarm size of 50 particles and a maximum of 100 iterations to ensure adequate exploration of the solution space.

These parameters were selected based on extensive preliminary simulations, where it was observed that the controller variables consistently converged within 100 iterations. Increasing the population size or iteration count beyond this point resulted in negligible improvement in performance, while increasing computational cost. Consequently, these values were adopted for both case studies to ensure efficient yet reliable optimization. Similar parameter choices are frequently reported in the nonlinear control literature and have demonstrated effective performance in our framework.

This optimization framework facilitates the design of a

robust state feedback controller that effectively accommodates system uncertainties while fulfilling predefined performance requirements.

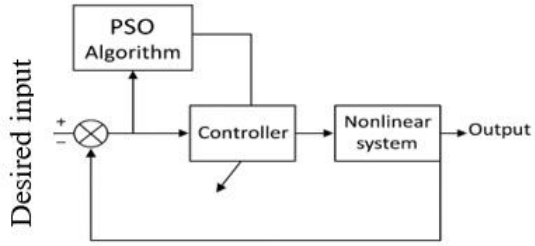

Figure 2. Layout of the proposed controller synthesized through Particle Swarm Optimization

5. CASE STUDIES AND CONTROLLER VALIDATION

This section investigates the effectiveness of the proposed control strategy through two nonlinear system case studies. The analysis focuses on comparing to assess the influence of the proposed controller, the systems' time-domain behavior is examined under two conditions: with the controller applied and without it. The first case study involves a nonlinear system that satisfies the matching condition, wherein the nonlinearities and control input coexist within the same state-space channel. Conversely, the second case examines a system that violates this condition, with nonlinear effects and control inputs acting through distinct channels. To ensure consistent numerical accuracy across all simulations, the MATLAB software was used with a fixed step fourth order Runge Kutta (ODE4) solver and a step size of 0.01 seconds.

5.1 Nonlinear pendulum system with parametric uncertainty

The following nonlinear pendulum system, characterized by uncertain parameters, is considered for analysis [17]:

$$\begin{gathered}\dot{x}_1(t) = x_2(t) \\ \dot{x}_2(t) = -\frac{g}{l}\sin(x_1) - \frac{k}{m}x_2(t) + \frac{1}{l}M(t)\cos(x_1) + \\ \frac{1}{ml^2}u(t) \\ y(t) = x_1(t)\end{gathered} \tag{38}$$

In this study, the variable $x_1(t)$ refers to the pendulum′s angular deviation from the vertical position, while $u(t)$ indicates the externally applied control torque, and g denotes the gravitational acceleration. The parameters $m, l, and\ k$ refer to the pendulum bob's mass, the rod length, and the friction coefficient, respectively, while $M(t)$ describes a bounded, time-dependent horizontal acceleration acting on the system. The parameters are listed in Table 1, which includes their nominal values. Furthermore, the pendulum rod is considered to be perfectly rigid with negligible mass, simplifying the dynamic modeling of the system. The reference signal is specified as $r(t) = 30e^{-0.1t}\sin(t)$, which serves as the desired angular trajectory for the pendulum. Prior to the application of the control strategy, a significant deviation is observed between the actual system response and the desired reference signal, as illustrated in Figure 3. This discrepancy highlights the necessity of designing an effective controller capable of minimizing tracking errors and ensuring the desired system performance under the influence of nonlinearities and external disturbances.

Table 1. Range and values of the system parameters [17]

Parameter	Unite	Minimum Bound	Default Value	Maximum Bound
m	Kg	0.5	1	1.5
l	m	0.9	1	1.1
k	Nms/ra	0	0.1	0.2
g	m/s^2	-	9.8	-
$M(t)$	rad/s^2	-1	0	1

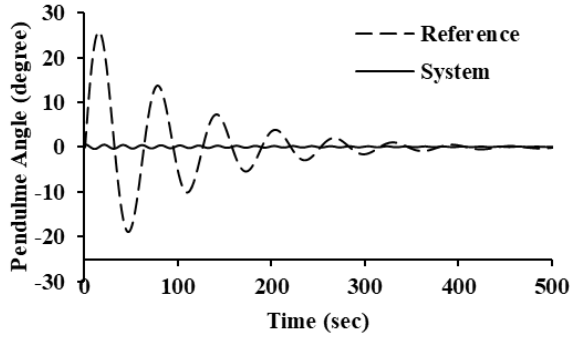

Figure 3. Time-domain response of the closed-loop system prior to implementing the controller design

The system's dynamic behavior can be expressed in the following reformulated form:

$$\begin{gathered}\dot{x}_1(t) = x_2(t) \\ \dot{x}_2(t) = -h_1\sin(x_1) - h_2x_2(t) + h_3\cos(x_1) \\ + h_4\,u(t) \\ y(t) = x_1(t)\end{gathered} \tag{39}$$

where, $h_1 = \frac{g}{l}, h_2 = \frac{k}{m}, h_3 = \frac{M(t)}{l}, h_4 = \frac{1}{ml^2}$ Subsequently, the uncertain coefficients $h_1, h_2,\ h_3,$ and h_4 are defined as follows:

$$\begin{aligned}h_1 &= \frac{g}{l_o} + \frac{g}{\delta_l} = 9.81 + \delta_{h_1} \\ h_2 &= \frac{k_o}{m_o} + \frac{\delta_k}{\delta_m} = 0.1 + \delta_{h_2} \\ h_3 &= \frac{M_o(t)}{l_o} + \frac{\delta_M}{\delta_l} = 0 + \delta_{h_3} \\ h_4 &= \frac{1}{m_o{l^2}_o} + \frac{1}{\delta_m{\delta_l}^2} = 1 + \delta_{h_4}\end{aligned} \tag{40}$$

Herein, the terms $\delta_l, \delta_k, \delta_m,$ and δ_M rdenote the discrepancies of the system's parameters from their corresponding nominal values, specifically $l_o, k_o, m_o,$ and $M_o(t)$. Consequently, the dynamic behavior of the system can be formally articulated as follows:

$$\begin{gathered}\dot{x}_1(t) = x_2(t) \\ \dot{x}_2(t) = -x_1 - 0.1x_2(t) + u(t) + \Delta_h \\ y(t) = x_1(t)\end{gathered} \tag{41}$$

where, $\Delta_h = x_1(t) - \left(9.81 + \delta_{h_1}\right)\sin(x_1) - \delta_{h_2}x_2(t) + \delta_{h_3}\cos(x_1) + \delta_{h_4}u(t)$.

All system perturbations clearly belong to the matched type, which removes the need for a diffeomorphic transformation.

Subsequently, the Particle Swarm Optimization (PSO) algorithm was employed as an optimization tool to determine

the most effective set of controller parameters, ensuring optimal performance of the control system. The PSO configuration settings are detailed in Table 2, while Table 3 presents the optimal parameter values along with their respective bounds. Upon completion of the optimization process, the positive-definite solution to the H-infinity Algebraic Riccati Equation (HIARE) was derived as follows:

$$P = \begin{bmatrix} 471.4968 & 34.9488 \\ 34.9488 & 3.5004 \end{bmatrix}$$

Subsequently, the gain matrix associated with the state feedback controller was calculated and is expressed as follows:

$$K = [-349.4876 \quad -35.0040]$$

Table 2. Configuration parameters of the PSO algorithm used in the pendulum case study

Optimization Setting	Value
Optimization problem dimensionality	5
Size of population	50
No. of iterations	100

Table 3. Optimized parameters with corresponding bounds

Optimally Tuned Parameter	Lower Bound	Upper Bound	Optimum Value
γ	0.5	10	0.736931
c_{11}	0	100	100
c_{12}	0	100	5.318
c_{21}	0	100	0.0001
c_{22}	0	100	1.576

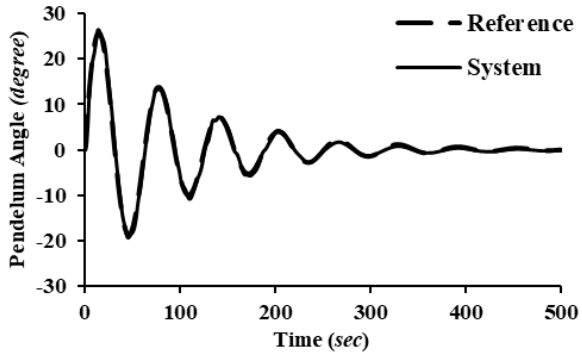

Figure 4. Time response of the pendulum angle in the nominal controlled system

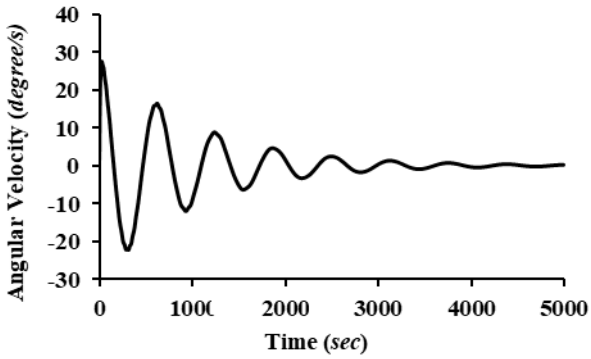

Figure 5. Angular velocity response of the nominal system under the designed controller

Figure 4 depicts the time response of the pendulum angle in the nominal controlled system. The results confirm that the angle closely tracks the desired reference signal, indicating the effectiveness of the proposed control strategy. In addition, Figure 5 depicted the tracking behavior of the angular velocity, further supporting the controller's capability in ensuring accurate state regulation. These outcomes collectively validate the capability of the controller to ensure nominal stability while achieving desirable dynamic performance. As shown in Figure 6, the control torque imposed on the system reflects the effort necessary to realize the intended dynamic behavior.

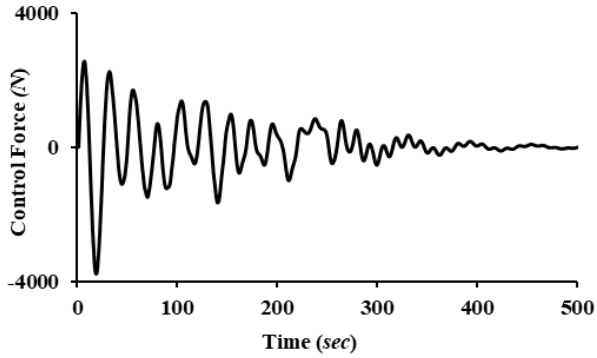

Figure 6. Behavior of the control torque

Furthermore, Figure 7 highlights the efficiency of the PSO optimization method in optimizing the parameters defining the controller. The figure demonstrates the convergence behavior of the objective function, reflecting the algorithm's efficiency in minimizing the integral square error (ISE), which was found to be 0.391 indicating a well-optimized solution.

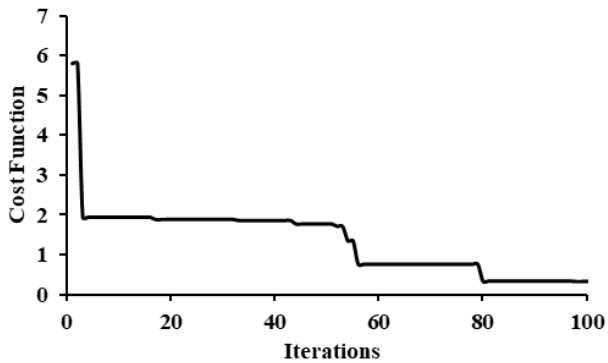

Figure 7. The convergence

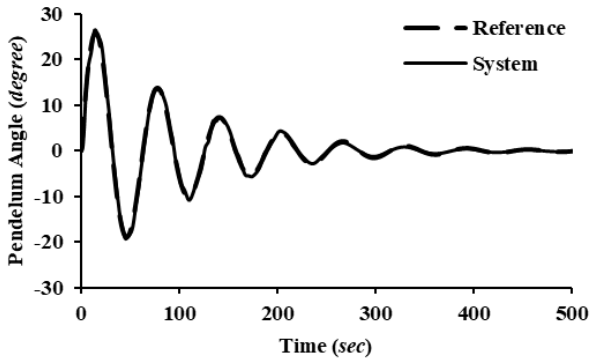

Figure 8. The trajectories of the pendulum angle for the controlled system under uncertain

The variation of the pendulum's angular position over time is illustrated in Figure 8 under the influence of parameter variations as defined in Table 1, while Figure 9 displays the corresponding angular velocity response. The consistency of these responses under perturbed conditions confirms the robustness and effectiveness of the proposed control strategy in preserving system stability and performance. Additionally, Figure 10 illustrates the complete temporal behavior of the nonlinear system following the application of the designed control scheme, clearly illustrating its capability to stabilize the system successfully.

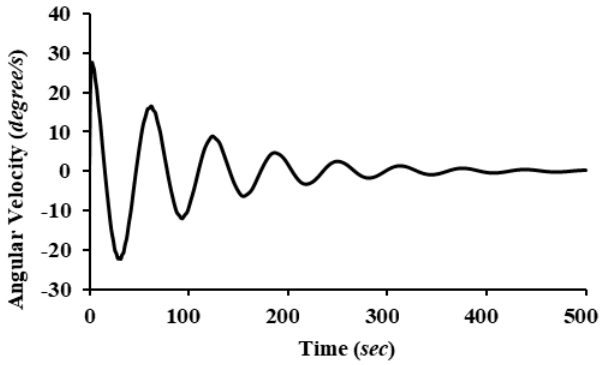

Figure 9. The trajectories of the angular velocity for the controlled system under uncertain

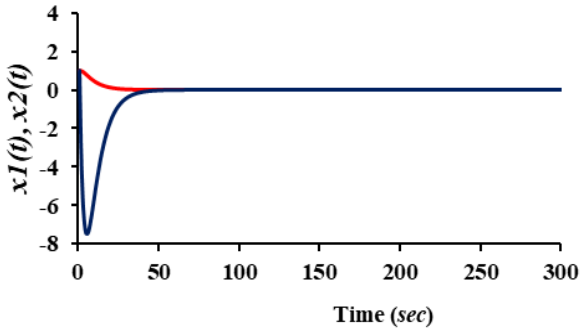

Figure 10. Stabilized trajectories of the nonlinear system states using the proposed control method

5.2 Nonlinear system with mismatched perturbation

The following nonlinear model is considered for control design [18]:

$$\begin{aligned} \dot{x}_1 &= \tan x_1 + x_2 \\ \dot{x}_2 &= c\, x_1 + u \\ y &= x_1 \end{aligned} \tag{42}$$

The variable c is considered an uncertain parameter, whose nominal value is 1, subject to a possible deviation of up to $\pm 90\%$ from this nominal value. Figures 11 and 12 depict the time-domain responses of the nonlinear system operating in both open-loop and closed-loop modes prior to applying the proposed control approach.

The results clearly indicate that the system remains unstable under both open-loop and closed-loop configurations, thereby necessitating the development of a suitable controller to ensure system stabilization and fulfill the desired performance criteria. Additionally, the nonlinear term $\tan(x_1)$ resides outside the control channel directly influenced by the input signal u, indicating that the matching condition is violated. Consequently, it becomes necessary to apply the diffeomorphic transformation specified in Eq. (9) to restructure the nonlinear system is reformulated into the standard controllable configuration as expressed in Eq. (12). This transformation is accomplished by substituting an alternative set of state variables as defined below:

Let:

$$z_1(t) = x_1(t), z_2(t) = \dot{z}_1(t) = \dot{x}_1(t) = \tan x_1 + x_2 \tag{43}$$

Then:

$$\dot{z}_2 = \sec^2(x_1)\dot{x}_1 + \dot{x}_2 \tag{44}$$

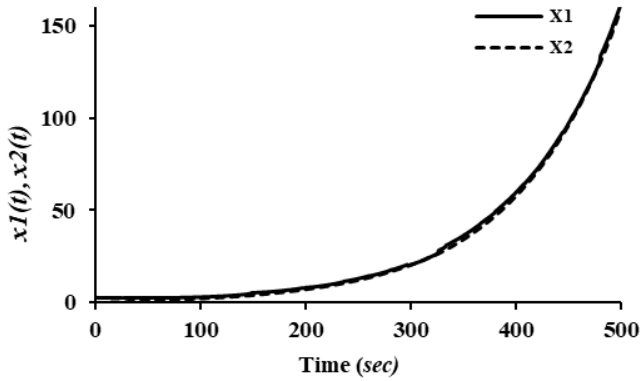

Figure 11. Time response of the nonlinear system under open-loop conditions before applying the proposed controller

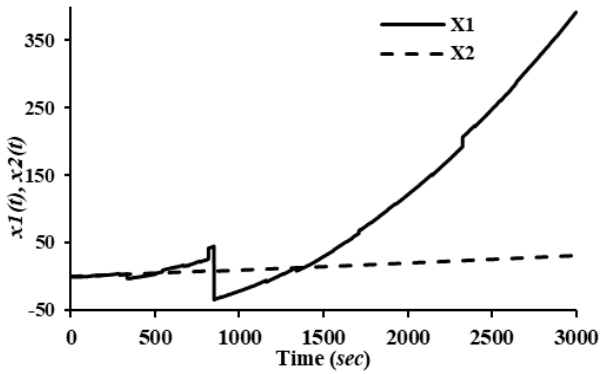

Figure 12. Time response of nonlinear system under closed-loop conditions before applying the proposed controller

From Eqs. (42) and (43), it is deduced that:

$$\dot{z}_2 = z_2 \sec^2(z_1) + c\, z_1 + u \tag{45}$$

The uncertain parameter a can be represented in the form of a multiplicative uncertainty term as follows:

$$c = c_o(1 + \delta_c) \tag{46}$$

where, c_o represents the nominal value of the uncertain parameter c, and δ_c denotes the relative percentage deviation from c_o.

Substituting Eq. (45) in Eq. (46), yields:

$$\dot{z}_2 = c_o\, z_1 + \delta_c c_o z_1 + z_2 \sec^2(z_1) + u \tag{47}$$

Accordingly, the system's state equation is reformulated into the following form:

$$\begin{aligned} \dot{z}_1(t) &= z_2(t) \\ \dot{z}_2(t) &= c_o z_1(t) + d(t) + u(t) \end{aligned} \tag{48}$$

where, $d(t) = \delta_c c_o z_1 + z_2 \sec^2(z_1)$

The system in z-plan then becomes:

$$\begin{bmatrix} \dot{z}_1(t) \\ \dot{z}_2(t) \end{bmatrix} = \begin{bmatrix} 0 & 1 \\ 1 & 0 \end{bmatrix} \begin{bmatrix} z_1(t) \\ z_2(t) \end{bmatrix} + \begin{bmatrix} 0 \\ 1 \end{bmatrix} d(t) + \begin{bmatrix} 0 \\ 1 \end{bmatrix} u(t) \tag{49}$$

The PSO algorithm was subsequently applied to compute the optimal control law. Table 4 outlines the PSO configuration parameters, while Table 5 lists the tuned controller variables, including their search bounds and resulting optimal values.

Table 4. Configuration parameters of the PSO algorithm used in the example 2

Optimization Setting	Value
Optimization problem dimensionality	5
Population size	50
Iterations No.	100

Table 5. Optimally tuned parameters and associated bounds

Optimally Tuned Parameter	Minimum Bound	Maximum Bound	Optimum Value
γ	0.5	10	0.5015
c_{11}	0	100	55
c_{12}	0	100	0.011
c_{21}	0	100	0.00011
c_{22}	0	100	0.000101

Following the determination of the optimal controller parameters via the PSO optimization, these values were substituted into the H-infinity Algebraic-Riccati-Equation (Eq. (37)). Solving this equation yielded a positive definite matrix P which defines the optimal state feedback gain and inherently ensures the stability of the closed-loop system. The computed matrix P is presented below:

$$P = 10^3 \begin{bmatrix} 0.5295 & 0.0287 \\ 0.0287 & 0.0031 \end{bmatrix}$$

Following this, the state feedback controller gain matrix is derived by applying Eq. (33), with the resulting matrix provided below:

$$K_c = [-209.425 \quad -36.8984]$$

As a result, the optimal control law formulated within the transformed *z-coordinate* space is expressed as follows:

$$u = -209.425 z_1 - 36.8984 z_2 \tag{50}$$

The control scheme is subsequently mapped from the z-coordinate space transformed back into the original x-coordinate space as follow:

$$u = -209.425 x_1 - 36.8984 \, tanx_1 - 36.8984 x_2 \tag{51}$$

Figure 13 demonstrate the proposed controller's robust tracking performance, characterized by minimal error and rapid convergence despite external disturbances. Figure 14 shows the stable state trajectory x_2 for the nominal system.

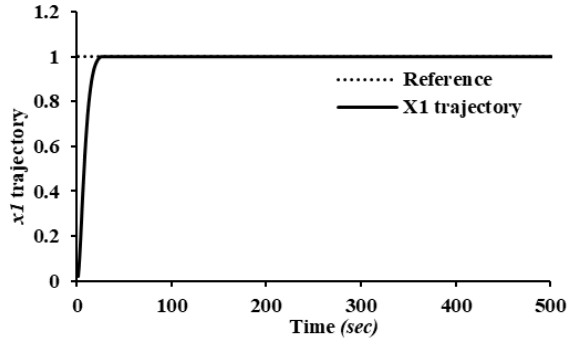

Figure 13. Tracking properties of the controlled nominal system

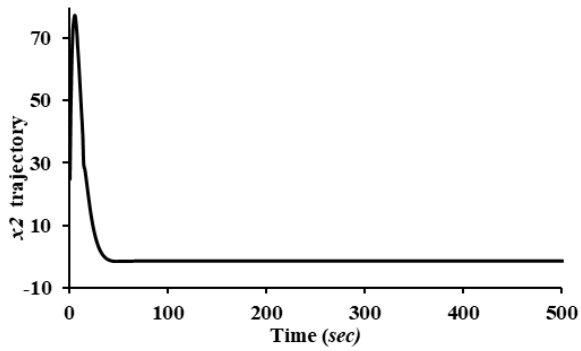

Figure 14. The behavior of x_2 trajectories of the controlled nominal system

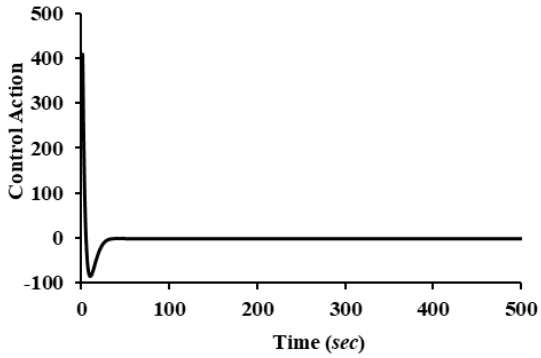

Figure 15. Performance of applied control

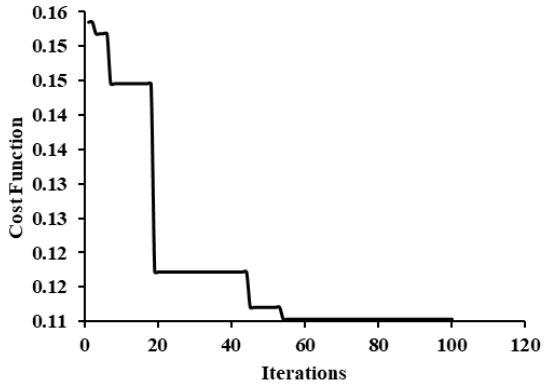

Figure 16. The convergence

Additionally, Figure 15 illustrates the applied control signal, verifying its feasibility and compliance with practical constraints. Additionally, Figure 16 show cases the capability of the PSO approach to effectively reduce the value of the objective function, demonstrating its ability to optimize control parameters efficiently, achieving an integral square error of 0.113.

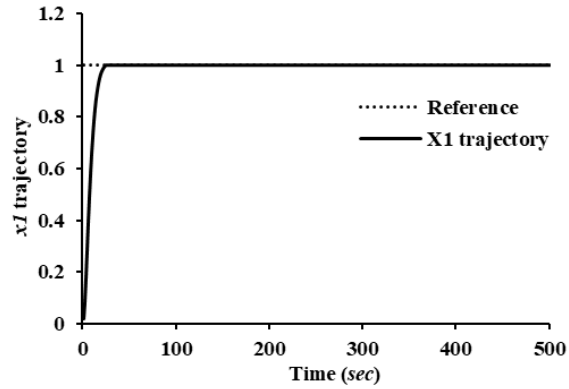

Figure 17. The output trajectory of the controlled system under uncertain

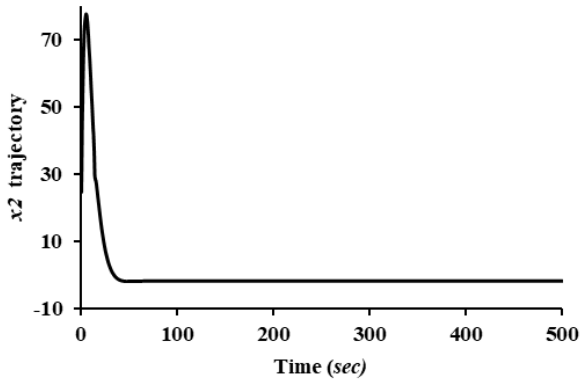

Figure 18. The behavior of x_2 trajectories of the controlled system under uncertain

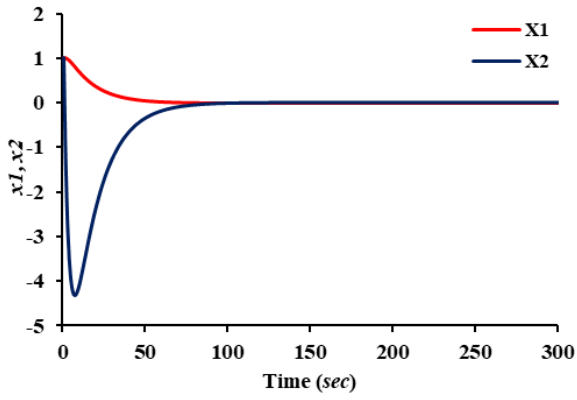

Figure 19. State trajectories of the nonlinear system stabilized through the implementation of the proposed control strategy

Figures 17 and 18 illustrate the evolution of the system states under the influence of parameter perturbations considered in this work. The observed responses confirm the capability of the proposed control scheme to preserve stability and ensure reliable performance, even in the presence of modeling uncertainties and parameter deviations.

Furthermore, Figure 19 illustrates the overall time-domain response of the nonlinear system under the designed controller, confirming successful stabilization and effective disturbance rejection across varying conditions.

6. CONCLUSIONS

This research endeavors to present the formulation of an optimal nonlinear control strategy, conceived within the robust H-infinity framework. This advanced control methodology is specifically designed to address and effectively manage two distinct classifications of nonlinear dynamical systems: this encompasses systems characterized by the satisfaction of a matching condition between the control input and the nonlinear disturbance terms, alongside those in which this condition is not met. The proposed controller successfully guaranteed asymptotic stability and achieved optimal tracking performance across both system types.

To facilitate precise tuning of controller parameters, the Particle Swarm Optimization (PSO) algorithm was employed, offering an efficient mechanism for exploring the design space. Furthermore, a diffeomorphic transformation was applied to reformulate the nonlinear systems into a controllable canonical form, allowing the nonlinearities and uncertainties to be consolidated into a perturbation vector treated as an additive disturbance to the nominal model.

The derivation of the optimal state-feedback gains was accomplished by obtaining a positive definite solution to the H-infinity Algebraic Riccati Equation (HIARE), thereby ensuring both robust stability and favorable closed-loop performance. The core contribution of this research lies in establishing a unified and systematically structured design methodology that is broadly applicable to various classes of nonlinear dynamical systems. This framework provides a practical, less computationally demanding, and more accessible alternative to the highly specialized and complex design strategies that dominate current literature.

Future research directions include extending the controller design to accommodate systems with higher degrees of uncertainty and parameter variations, where adaptive or enhanced robust control strategies may further improve performance and resilience.

REFERENCES

[1] Chatavi, M., Vu, M.T., Mobayen, S., Fekih, A. (2022). H_∞ robust LMI-based nonlinear state feedback controller of uncertain nonlinear systems with external disturbances. Mathematics, 10(19): 3518. https://doi.org/10.3390/math10193518

[2] Tayyeh, I.F., Ali, H.I. (2022). Full state feedback H-infinity controller design for nonlinear systems. Journal Européen des Systèmes Automatisés, 55(4): 503-509. https://doi.org/10.18280/jesa.550409

[3] Saravanakumar, R., Ali, M.S., Huang, H. (2018). Robust H_∞ state-feedback control for nonlinear uncertain systems with mixed time-varying delays. International Journal of Control, Automation and Systems, 16(1): 215-223. https://doi.org/10.1007/s12555-017-9263-6

[4] Wu, Z., Xiao, X. (2015). State feedback H_∞ control of power units based on an improved particle swarm

optimization. Mathematical Problems in Engineering, 2015(1): 928343. https://doi.org/10.1155/2015/928343
[5] Sathya, S., Rajendran, A.G. (2020). Optimal tuning of robust H_∞ controller for nonlinear systems using PSO. International Journal of Intelligent Engineering and Systems, 13(2): 239-248. https://doi.org/10.22266/ijies2020.0430.23
[6] Yang, X., Yuan, J., Yuan, J., Mao, H. (2007). A modified particle swarm optimizer with dynamic adaptation. Applied Mathematics and Computation, 189(2): 1205-1213. https://doi.org/10.1016/j.amc.2006.12.045
[7] Ali, M.H.M.H.I., Noor, S.B.M., Bashi, S.M. (2010). Design of H-infinity based robust control algorithms using particle swarm optimization method. Mediterranean Journal of Measurement and Control, 6(2): 70-81.
[8] Zirkohi, M.M., Fateh, M.M., Shoorehdeli, M.A. (2013). Type-2 fuzzy control for a flexible-joint robot using voltage control strategy. International Journal of Automation and Computing, 10(3): 242-255. https://doi.org/10.1007/s11633-013-0717-x
[9] Qaraawy, S., Ali, H., Mahmood, A. (2012). Particle Swarm Optimization based robust controller for congestion avoidance in computer networks. In 2012 International Conference on Future Communication Networks, Baghdad, Iraq, pp. 18-22. https://doi.org/10.1109/ICFCN.2012.6206865
[10] Ali, H.I., Hadi, M.A. (2020). Optimal nonlinear controller design for different classes of nonlinear systems using black hole optimization method. Arabian Journal for Science and Engineering, 45(8): 7033-7053. https://doi.org/10.1007/s13369-020-04650-z
[11] Hatamlou, A. (2013). Black hole: A new heuristic optimization approach for data clustering. Information Sciences, 222: 175-184. https://doi.org/10.1016/j.ins.2012.08.023
[12] Shareef, Z.M., Ali, H.I. (2018). Full state feedack H2 and H-infinity controllers design for a two wheeled inverted pendulum system. Engineering and Technology Journal, 36(10A): 1110-1121. https://doi.org/10.30684/etj.36.10A.12
[13] Sinha, A. (2007). Linear Systems: Optimal and Robust Control. CRC Press, Taylor & Francis Group, New York.
[14] Khalil, H.K. (2002). Nonlinear Systems. 3rd Ed., Prentice Hall, Upper Saddle River, New Jersey.
[15] Mahmood, A.H., Ali, H.I. (2021). Optimal H-infinity integral dynamic state feedback model reference controller design for nonlinear systems. Arabian Journal for Science and Engineering, 46(10): 10171-10184. https://doi.org/10.1007/s13369-021-05447-4
[16] Ibrahim, I.H., Ali, H.I. (2021). Quantitative PID controller design using Black Hole optimization for ball and beam system. Iraqi Journal of Computers, Communications, Control and Systems Engineering, 21(3): 65-75. https://doi.org/10.33103/uot.ijccce.21.3.6
[17] Khalil, H.K. (2002). Nonlinear Systems. 3rd Ed. Upper Saddle River, NJ: Prentice-Hall.
[18] Tayyeh, I.F., Ali, H.I. (2022). Full state feedback H-infinity controller design for nonlinear systems. Journal Européen des Systèmes Automatisés, 55(4): 503-509. https://doi.org/10.18280/jesa.550409